# Evaluation of Phoswich Well Detectors for Radioxenon Monitoring

Wolfgang Hennig, Hui Tan, William K. Warburton, Anthony Fallu-Labruyere, Konstantin Sabourov, Justin I. McIntyre, Matthew W. Cooper, and Anshel Gleyzer

***Abstract*–Systems to monitor radioactive xenon in the atmosphere, part of an international network to detect nuclear weapons testing, often employ beta-gamma coincidence measurements to increase sensitivity. Existing coincidence systems use separate detectors for beta and gamma radiation and thus require several electronics readout channels that are cumbersome to set up and calibrate. To simplify such systems, we designed phoswich well detectors which require only a single readout channel and evaluated their performance for radioxenon detection.**

## I. Introduction

Devices to measure the amount of radioactive xenon in the atmosphere, part of the International Monitoring System established by the Comprehensive Nuclear-Test-Ban Treaty to detect nuclear weapons testing, have been installed in several locations around the world. These devices, e.g. the Automated Radioxenon Sampler and Analyzer (ARSA) [1] or the Swedish Automatic Unit for Noble gas Acquisition (SAUNA) [2], extract Xe from large volumes of air and then measure its radioactivity in an extremely low background counter. Since the Xe isotopes of interest all emit one or more beta particles or conversion electrons simultaneously with one or more gamma rays or X-rays, beta-gamma coincidence can be used effectively to suppress the natural background.

Currently, the devices use time based coincidence detection with separate detectors for beta and gamma radiation, which requires several channels of photomultiplier tubes (PMTs) and readout electronics. This leads to complex systems that require careful gain matching and calibration. Phoswich detectors have been studied as a potential simpler solution [3], [4], using pulse shape analysis (PSA) to detect coincidences in the signal from a single PMT. Using Monte-Carlo simulations, we previously studied several possible designs of phoswich well detectors that could be used as drop-in replacements for the existing ARSA detector unit [5]. The objective of the work presented in this paper was to build prototypes of the more promising designs and characterize their performance, i.e. determine properties such as energy resolution, coincidence detection efficiency, background rejection and the ability to separate beta only, gamma only, and coincidence events.

Manuscript received November 16, 2007. This work was supported by the U.S. Department of Energy under Grant No. DE-FG02-04ER84121

W. Hennig, H.Tan, W.K. Warburton. A. Fallu-Labruyere, and K. Sabourov are with XIA LLC, Hayward, CA 94544 USA (e-mail: whennig@xia.com)

J. I. McIntyre and M. W. Cooper are with Pacific Northwest National Laboratory, Richland, WA 99352 USA

A. Gleyzer is with PhotoPeak, Inc, Chagrin Falls, Ohio 44023 USA

## II. Measurements

Two detector prototypes, named PW2 and PW3, were built. They both consist of a 2.54 cm diameter BC-404 plastic cell (absorbing betas) enclosed in and optically coupled to a 7.62 cm diameter CsI(Tl) crystal (absorbing gammas), but differ in detector geometry as shown in Fig. 1. PW2 is easier to manufacture, but due to the cut in CsI parallel to the PMT window, the light collection and thus energy resolution are degraded [5]. The geometry of PW3 has the best light collection and resolution among all designs studied in the simulations, but is more difficult to manufacture. The detector as currently built has a PMT with low gain and relatively high noise. Thus any results presented here for PW3 represent a detector that has not yet been fully optimized.

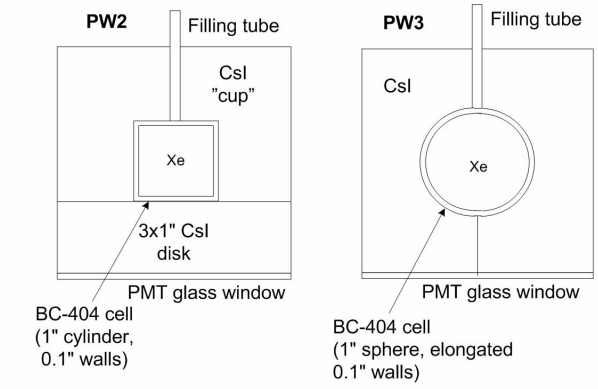


Fig. 1. Geometries of phoswich well detectors studied. Left: 1st well prototype (PW2); right: 2nd well prototype (PW3).

### A. Energy Resolution

For PW2, we obtain an overall resolution of ~12% full width at half maximum (FWHM) for 662 keV gamma rays from a $^{137}$Cs source outside the detector. Closer analysis shows that there are actually 2 overlapping peaks with resolutions of ~7% and ~9% FWHM, their relative intensity varying according to location of the source. We attribute this to the different light collection efficiency in the two sections of the CsI crystal [5]. For PW3, the resolution is ~9%, a single peak independent of the location of the source. Resolutions for other sources and energies are given in Table 1. Note that for low energies, the resolution of PW2 becomes equal to PW3, because the fixed ~6% separation of the 2 peaks from the two CsI crystal segments becomes negligible when added in quadrature with other peak broadening effects, such as photostatistics. Due to the noisy, low gain PMT currently used

with PW3, its resolution is *worse* than PW2 at very low energies. These measurements will be repeated soon with a replaced PMT. Preliminary results from two production detector in the same geometry as PW3 are ~8.4% FWHM at 662 keV and ~20% FWHM at 60 keV.

TABLE I
ENERGY RESOLUTION (FWHM) OF PW2 AND PW3. FOR EXTERNAL SOURCES, NO PSA TO SEPARATE EVENT TYPES WAS APPLIED. ARSA VALUES FROM [7]. VALUES IN () ARE PRELIMINARY, TO BE REPEATED WITH A REPLACED PMT.

| Resolution | PW2 | PW3 | ARSA | Notes |
|---|---|---|---|---|
| Ec = 662keV (external $^{137}$Cs) | 12% | 9% | 12% | PW2: 2 peaks, ~7% and ~9% |
| Ec = 609keV (internal $^{222}$Rn) | 12% | 10% | | Coincidence events only |
| Ec = 120keV (external $^{57}$Co) | 16% | 17% | 22% | |
| Ec = 60keV<br>Ec = 26keV (external $^{241}$Am) | 18%<br>31% | (23%)<br>(36%) | | PW3: small signal close to noise with this PMT |
| Ec = 30keV<br>Ep = 129keV (internal $^{131m/133}$Xe) | 35%<br>26% | (47%)<br>(43%) | 32%<br>37% | PW3: small signal close to noise with this PMT |

### B. *Energy Histograms*

Using the fact that interactions in the plastic scintillator generates very fast pulses (< 100 ns) while the CsI pulses are slow (several microseconds), each pulse from the phoswich detector is processed to extract the portion of energy deposited in CsI and plastic scintillators [4]. Fig. 2 shows 2D histograms of CsI energy (Ec) vs. plastic energy (Ep) for measurements with a $^{222}$Rn source (NIST SRM 4974). The 2D histograms show horizontal lines of coincidence events from beta particles (Ep varies) and photons (peaks at Ec = 80 keV, 241 keV, 295 keV, 351 keV and 609 keV) from $^{222}$Rn daughter products. The 80 keV line is offset in Ep as a conversion electron with constant energy emitted at the same time as the variable energy beta particle. The energy resolution of Ec for the 609 keV coincidence line is about 11.8% FWHM in PW2, with a noticeable shoulder or second peak towards higher energies (see Fig. 3). For PW3, the resolution is about 10.2% with no shoulder

In both detectors, but less pronounced in PW3, there is also a rising diagonal line starting at Ec ~ 0 keV, Ep ~ 150 keV. The "peaks" along the line – allowing for a different energy scale and non-linearity at low energies for heavy charged particles [6] – match the alpha energies in the $^{222}$Rn decay chain. We thus conclude that these events are alpha particles, generating a slightly different pulse shape (slower decay) than electrons or photons when interacting with the plastic scintillator. The PSA algorithms, in their current form, interpret the slower decay as a contribution of a slow CsI pulse and thus compute a component in Ec proportional to the pulse height. Because Rn is removed from the sample in Xe monitoring measurements to minimize interference in the 80 keV line, there should then be no significant interference from alpha particles either. On the other hand, it is also possible to modify the PSA algorithms to detect and remove alpha pulses from the recorded data, e.g., by shape-matching fits, measuring the fall time or additional sums over characteristic intervals in the pulse.

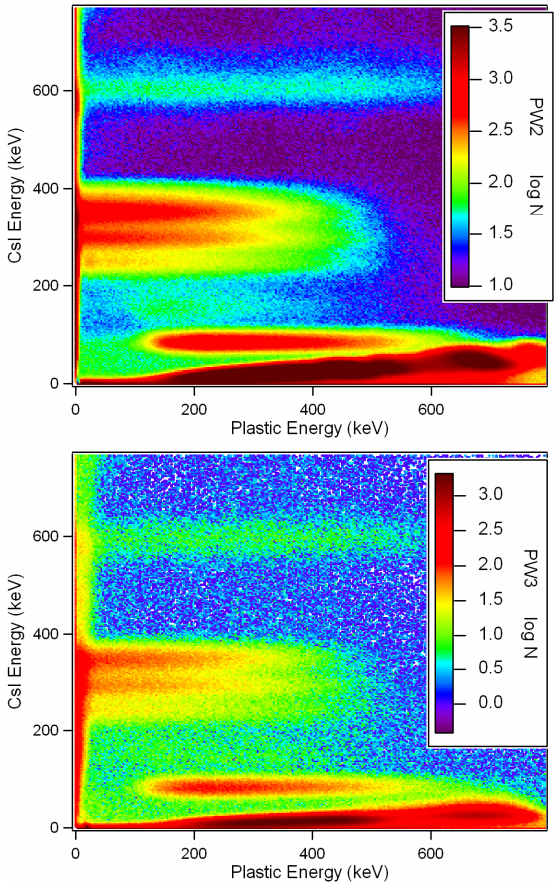


Fig. 2. 2D energy histograms for PW2 (top) and PW3 (bottom) for measurements with a $^{222}$Rn source. Note the color scales differ due to different number of counts in each measurement.

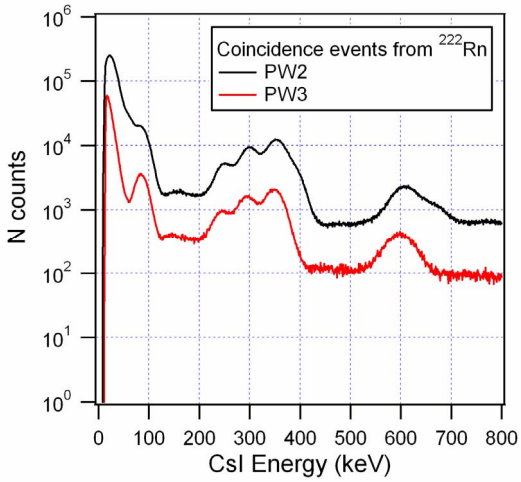


Fig. 3. Histograms of energy deposited in CsI (in coincidence events only) for PW2 and PW3 in measurements with a $^{222}$Rn source. The shoulders in the peaks of PW2 at 241-351 keV and 609 keV are due to the non-uniform light collection in different sections of the detector.

Fig. 4 shows 2D histograms of Ec vs. Ep for measurements with a $^{131m/133g}$Xe source, featuring two peaks for conversion electrons from $^{131m}$Xe (Ec;Ep = 0;160 keV and 30;129 keV) and two lines of beta/photon coincidences from $^{133g}$Xe at Ec = 30 keV and Ec = 80 keV. The resolution at Ec = 30 keV is ~35% for PW2 and ~48% for PW3. In measurements with $^{131m}$Xe, the resolution for coincidence events for PW2 is ~29% at Ep = 129 keV.

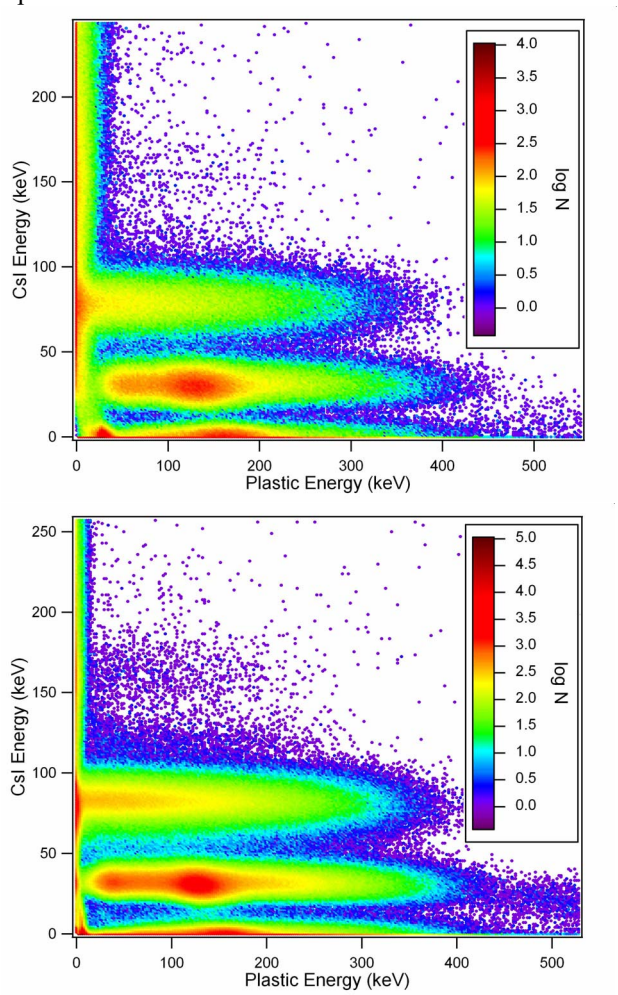


Fig. 4. 2D energy histograms for PW2 (top) and PW3 (bottom) for measurements with a $^{131m/133g}$Xe source.

### C. Background

In monitoring applications, the samples of radioxenon collected are very small, so the background count rate of the detector has to be as low as possible. In a lead enclosure (lead wall thickness is 5.08 cm with an additional 1.27cm inner lining with Oxygen-Free High Conductivity [OFHC] copper), we measure an overall rate of 4-5 counts/s for PW2, of which ~0.05 counts/s are coincidences. The overall rate for PW3 is 3-7 counts/s, of which ~0.04-0.09 counts/s are coincidences. The ARSA detector, consisting of two much bigger NaI crystals, has an overall background rate of ~30 counts/s of which 0.1 counts/s are coincident, i.e., the background in Xe regions of interest is can be up to a factor of 2 higher.

## III. Characterization

### A. Coincidence Detection Efficiency

We define the coincidence detection efficiency at a given energy as the number of net coincidence counts in the peak, divided by the number of all net counts in the peak. From a $^{131m}$Xe measurement for PW2, we obtain the coincidence detection efficiency for the 30keV peak as 97.6%. A small fraction (about 1.5%) of coincidence events fall outside the main peak; most of these can be attributed to Compton scattering of ~160 keV gamma rays from plastic to CsI or vice versa. For a given conversion electron energy, this fraction depends primarily on the wall thickness of the plastic cell [5].

Measurements with a mixture of $^{131m}$Xe and $^{133g}$Xe result in an estimated coincidence detection efficiency of 98.5% for PW2 and 98.9% for PW3 at 30 keV. As expected, the values are very similar since the difference in detector design affects mostly the light collection, not the absorption of radiation.

### B. Background Rejection

Adding an external $^{137}$Cs source as "controlled background" in measurements with PW2 in the lead enclosure, we find an increase in overall count rate of 77 counts/s (with this particular source and distance). Most of the $^{137}$Cs photons interact only with the CsI; however a small fraction will Compton scatter from the CsI to the plastic or vice versa, generating coincidence events. The increase in the coincidence count rate is only 0.48 counts/s, i.e. 0.6% of the overall increase. Thus the background rejection rate (background represented by a $^{137}$Cs source) is 99.4% for PW2. For PW3, we compute a background rejection rate of 99.2% from a measurement with a $^{137}$Cs source adding 526 counts/s.

### C. Ability to Separate Event Types

Events are processed one by one with PSA algorithms to categorize them as CsI only (gamma), plastic only (beta) or both (coincidence) based on user defined thresholds in energy and signal rise time. Close inspection of a subset of events indicate an error rate of ~1% in each category due to the automated pulse shape analysis, for example 1% of the events categorized as coincidence events are actually CsI only events or plastic only events. The most common reasons for mis-categorization are noise spikes in very low energy events and random coincidences (e.g., 2 plastic pulses following each other closely), and most of the mis-categorized events thus fall close to the origin in the 2D histogram, outside the region of interest for Xe isotopes.

From the resolution of the coincidence peak and the distribution of beta only and gamma only events along the axes in the 2D histogram, we estimate the minimum detectable coincidence energy for PW2 to be Ec ~13 keV and Ep ~25 keV in the plastic, which means that lower energies are not clearly distinguishable from CsI only or plastic only events, respectively. A setup using separate, optically isolated detectors may have thresholds of 10-20 keV, thus resulting in a comparable minimum detectable coincidence energy coincidences of interest occur at such low energies.

## IV. Gain Calibration and Drift

Quantitative isotope analysis for radioxenon monitoring relies on measuring the number of counts in specific regions of interest in the 2D histogram. Therefore, in repeated measurements and over long periods of time, the detector system has to deliver spectra with a fixed range in both beta energy and gamma energy (exact same scale keV/bin).

For a single detector (one scintillator with PMT), the deposited energy can be assumed to be proportional to the measured pulse height, and thus a single gain calibration constant is usually sufficient to histogram pulses into an energy spectrum. However, even when holding external environmental factors such as temperature and magnetic field constant, gains may drift over time. Therefore the calibration constant has to be verified periodically and either the constant or the PMT gain has to be adjusted to correct for any gain changes.

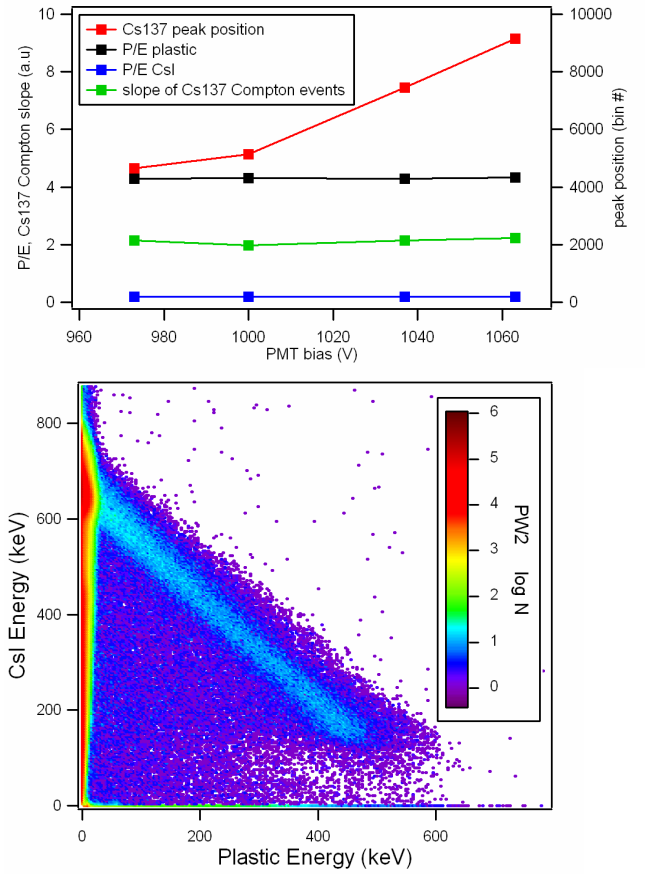


Fig. 5. Top: Variation of peak position and P/E processing constants with PMT bias (i.e., gain). Bottom: 2D energy histogram for a $^{137}$Cs source. The slope of the full energy Compton events (line of light blue pixels) is plotted in green in the top graph for different values of PMT bias. Processing constants and Compton slope do not depend on PMT gain, simplifying calibration.

In the phoswich detector system, the plastic and CsI energies are derived by PSA algorithms from the measured pulse height (called E) and a sum accumulated over the initial portion of the pulse (called P). Both E and P depend on the gain of the detector as in a single detector. The algorithms rely on two processing constants, essentially the ratios P/E for plastic only and CsI only events. These ratios are detector constants depending on the pulse shape and relative light output of the plastic and CsI scintillators. They are easily determined in calibration measurements with beta/gamma emitting reference sources such as $^{222}$Rn and $^{131m}$Xe, but even a typical $^{137}$Cs source generates in a few minutes a sufficient number of plastic only pulses for the calibration. Most importantly, the P/E ratios *do not* depend on the gain of the detector, since both fast and slow components of the pulse are equally affected by any gain changes. This can be seen in Fig. 5 (top), plotting the P/E ratios and the position of the 662 keV peak from $^{137}$Cs as a function of PMT bias (i.e., gain). While the peak position shifts to higher bins at higher gains, the P/E ratios remain constant (the standard deviation of measured P/E ratios is 0.5% for the plastic scintillator and 0.2% for CsI). Consequently, in measurements with different gains, the energy scales of Ep and Ec both change by the same factor. The slope fitted to the Compton scattered events in the 2D histogram—the light blue line in Fig. 5 (bottom)—remains a constant within the precision of the measurement.

In practice this means that even though the PSA introduces additional processing constants to determine the individual energies, only the overall gain calibration has to be verified and adjusted periodically. The processing constants have to be determined only once, for example at the production or installation of the detector. In periodic adjustments for gain, only a single measurement with a $^{137}$Cs reference source, as simple as determining the peak position of the 662 keV peak, is required to calibrate the scales of both energy axes. Alternatively, if there are well-defined peaks in the naturally occurring singles background, they might also be used to monitor and stabilize the PMT's gain.

In contrast, the existing ARSA detector system has separate beta and gamma detectors and uses multiple PMTs to read out the same scintillator. Therefore, during calibration these shared PMTs first have to be adjusted to have the exact same gain, and then for each scintillator a gain calibration constant has to be determined. This amounts to 6 gain matches and 6 gain constants for 4 sample cells compared to only 1 gain dependent calibration constant per sample cell for the phoswich detector. The resulting simplifications in field operation that are expected to result from this reduction in necessary calibration measurements have, naturally, been a major driving force for the development of this phoswich technology.

The magnitude of drifts for the phoswich detector can be seen in Fig. 6, showing peak positions in Xe measurements accumulated in 1-2 hour sub-runs over more than 30 days without gain adjustment. The 80, 129, and ~160 keV peaks shift by about ±1% for PW2 (PW3: about +2/-4%). The "30 keV" peak is a combination of a 31 keV line from $^{133g}$Xe and a 30 keV line from $^{131m}$Xe, so its position shifts by ~3% as the $^{133g}$Xe decays. Since only one detector/PMT is used, gamma and beta peaks drift in the same manner, e.g. the relative drift between PW2's 160 keV and 80 keV peaks (smoothed) is below ±0.25%, the absolute drift about 0.5%. This confirms

that the same gain calibration adjustment can be applied to all energy axes.

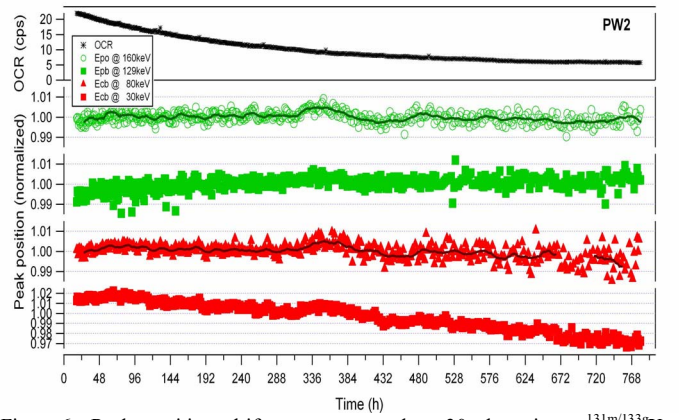


Fig. 6. Peak position drifts over more than 30 days in a $^{131m/133g}$Xe measurement. (Statistics for the 80 keV peak worsens and the "30 keV" peak shifts from 31keV to 30 keV as the $^{133g}$Xe decays.) Beta and gamma peaks drift in the same manner as they are derived from the same PMT/electronics channel, e.g. see "hump" at ~336 hours.

## V. Conclusion

In summary, we have built and evaluated two phoswich well detector prototypes. Overall, their performance is comparable to the existing ARSA detector: the background is somewhat lower, the resolution slightly better or equal, and the energy thresholds for coincidence detection somewhat higher. PW3 has better energy resolution, as expected from previous simulations, but more tests are necessary with a better PMT to complete its evaluation.

The key advantage of the phoswich detectors is their much simpler calibration, since the single PMT requires only periodic calibration of one gain dependent constant per sample cell instead of three, and the beta energy can be scaled from the peak position of the $^{137}$Cs gamma peak.

Future work will include the long term evaluation of two additional phoswich detectors made in the same geometry as PW3 at various laboratories involved in radioxenon monitoring.

## References


[1] P.L. Reeder, T.W. Bowyer, and R. W. Perkins, "Beta-gamma counting system for Xe fission products", Journal of Radioanalytical and Nuclear Chemistry 235: (1–2), 89–94. (1998).

[2] A. Ringbom, T. Larson, A. Axelsson, K. Elmgren, C. Johansson, "SAUNA—a system for automatic sampling, processing, and analysis of radioactive xenon", Nuclear Instruments and Methods in Physics Research A 508, 542–553 (2003).

[3] J.H. Ely, C. E. Aalseth, J. C. Hayes, T. R. Heimbigner, J. I. McIntyre, H.S. Miley, M. E. Panisko, and M. Ripplinger. "Novel beta-gamma coincidence measurements using phoswich detectors", in Proceedings of the 25th Seismic Research Review—Nuclear Explosion Monitoring: Building the Knowledge Base, LA-UR-06-6029, Vol. 2, pp. 533–541 (2003).

[4] W. Hennig, H.Tan, W. K. Warburton, and J. I. McIntyre. "Single channel beta-gamma coincidence detection of radioactive Xenon using digital pulse shape analysis of phoswich detector signals", IEEE Transactions on Nuclear Science 53: (2) p. 620 (2006).

[5] W. Hennig, H.Tan, A. Fallu-Labruyere, W. K. Warburton, J. I. McIntyre and A. Gleyzer, "Design of a phoswich well detector for radioxenon monitoring", in Proceedings of the 28th Seismic Research Review: Ground Based Nuclear Explosion Monitoring Technologies, LA-UR-06-5471, Vol. 2, pp. 801–810 (2006).

[6] G. F. Knoll, Radiation Detection and Measurement, J Wiley & Sons, Inc. (2000), Chapter 8

[7] P.L. Reeder, T.W. Bowyer, J. I. McIntyre, W.K. Pitts, A. Ringbom, and C. Johansson "Gain calibration of β/γ coincidence spectrometer for automated radioxenon analysis", Nuclear Instruments and Methods in Physics Research A 521, 586–599 (2004).